# Chasing Uptake

Baranov, Maksim V.; Olea, Rodica Alis; van den Bogaart, Geert

*Published in:*
Trends in Cell Biology

*DOI:*
10.1016/j.tcb.2019.05.006



*Publication date:*
2019

Trends in Cell Biology

CellPress
REVIEWS

Review

# Chasing Uptake: Super-Resolution Microscopy in Endocytosis and Phagocytosis

Maksim V. Baranov,[1] Rodica Alis Olea,[2] and Geert van den Bogaart [1,3,*]

**Since their invention about two decades ago, super-resolution microscopes have become a method of choice in cell biology. Owing to a spatial resolution below 50 nm, smaller than the size of most organelles, and an order of magnitude better than the diffraction limit of conventional light microscopes, super-resolution microscopy is a powerful technique for resolving intracellular trafficking. In this review we discuss discoveries in endocytosis and phagocytosis that have been made possible by super-resolution microscopy – from uptake at the plasma membrane, endocytic coat formation, and cytoskeletal rearrangements to endosomal maturation. The detailed visualization of the diverse molecular assemblies that mediate endocytic uptake will provide a better understanding of how cells ingest extracellular material.**

## Highlights

Super-resolution microscopy is widely available to most cell biologists and has become the method of choice for studying endocytic and phagocytic trafficking.

Current live imaging techniques allow 3D super-resolution microscopy with a temporal resolution of seconds to visualize uptake and trafficking processes at the whole-cell level.

Quantification strategies combined with super-resolution microscopy have enabled a quantitative understanding of receptor clustering, the appearance of signaling lipids, and the dynamics of F-actin assembly on endosomes and phagosomes.

Super-resolution microscopy is often combined with techniques such as electron microscopy and TIRF to enable more accurate localization of endocytic proteins in relation to stage of uptake, membrane curvature, and protein–protein interactions.

Although generally of lower spatial resolution compared with other super-resolution microscopy techniques, structured illumination microscopy has at present yielded most new insights in endocytic trafficking because it combines improved spatial resolution with a reasonably high temporal resolution and can be readily used for live cell imaging applications.

## Early Visualization of the Cellular Trafficking System

The mystery of how cells organize endocytic trafficking system has been extensively studied [1–4]. Endocytosis and phagocytosis (reviewed in [5]) are evolutionarily conserved mechanisms of internalization of solutes or small particles (endocytosis) or large particles sized above ~0.5 μm (phagocytosis). Insight into endocytic and phagocytic trafficking provides understanding of disease mechanisms because they are essential for many physiological processes, including nutrient uptake, immune clearance of pathogens, and the removal of apoptotic cells [3]. They are highly dynamic processes that begin with clustering of specialized membrane receptors at the site of uptake [6], followed by the assembly of coat proteins such as clathrin (endocytosis) or the engulfment of a particle by rapid actin rearrangements into protrusive pseudopodia (phagocytosis). Alternatively, many receptors are captured by pre-existing clathrin sites, thereby facilitating their uptake. Endocytosis and phagocytosis are orchestrated by the membrane composition, coat proteins, the **F-actin** (see Glossary) cytoskeleton, and membrane fission proteins such as dynamin [7]. After their formation, endosomes and phagosomes undergo a mechanistically similar maturation process in which they are transported via microtubules to the **microtubule organizing center (MTOC)** and gradually convert into late endo/phagosomes and finally into lysosomes [8].

Our current understanding of the nanoscale organization and morphology of endosomes and phagosomes stems mainly from **electron microscopy (EM)**. From this technique, we know that cells are very crowded, containing organelles of sizes ranging from tens of nanometers for small trafficking vesicles to up to several micrometers for the nucleus and large phagosomes (Figure 1A). Moreover, many organelles have a highly complex and dynamic morphology, such as the heterogeneous network of recycling endosomes. However, EM can only be used on fixed or frozen material and cannot follow dynamic processes in living cells, making this technique unsuitable for research questions related to dynamic alterations and stoichiometries of molecular assemblies. Live cell imaging is feasible with optical microscopy, but, owing to their small size, individual organelles are often impossible to resolve with conventional optical microscopy. Starting about two decades ago, the development of super-resolution microscopy techniques, including

[1]Department of Molecular Immunology, Groningen Biomolecular Sciences and Biotechnology Institute, University of Groningen, Groningen, The Netherlands
[2]Nanoscopy for Nanomedicine Group, Institute of Bioengineering of Catalonia, The Barcelona Institute of Science and Technology, Carrer Baldiri Reixac 15–21, 08024 Barcelona, Spain

stimulated emission depletion (STED) (Figure 1B), single-molecule localization microscopy (SMLM), structured illumination microscopy (SIM), and lattice light sheet microscopy (LLSM), is helping to overcome this problem (Box 1 for more information on each super-resolution technique) [9–16]. It is therefore no surprise that these techniques have provided crucial information on trafficking, particularly on exocytosis in neurons, neuroendocrine cells, and immune cells [14,17,18]. This review aims to provide an overview of the breakthrough discoveries that have been enabled by super-resolution microscopy specifically in endocytosis and phagocytosis.

[3]Department of Tumor Immunology, Radboud University Medical Center, Radboud Institute for Molecular Life Sciences, Geert Grooteplein 28, 6525GA Nijmegen, The Netherlands

*Correspondence:
G.van.den.Bogaart@rug.nl
(G. van den Bogaart).

## Organization of Endocytic Receptors at the Plasma Membrane

The clustering of endocytic receptors in distinct regions of the plasma membrane allows the localized uptake of material. SIM microscopy revealed that receptor-mediated caveolar and clathrin-coated vesicular uptake and nonspecific endocytosis occur at separate locations on the plasma membrane [19–21]. The spatial clustering and segregation of these different forms of endocytosis likely enable more efficient uptake and might facilitate the differential sorting of cargoes into different types of endosomes. In addition, receptor clustering can promote downstream signaling, for instance by oligomerization of kinase domains. Indeed, a SIM microscopy study in human macrophages showed that the Fc receptor FcγRIIA must diffuse laterally to become activated upon clustering by multivalent targets [22]. SMLM revealed that such clusters are approximately ~70 nm in size and contain ~100 Fc receptors [23], and that they locate adjacent to clusters enriched in the inhibitor of phagocytosis signal regulatory protein α (SIRPα) [24]. SMLM microscopy revealed that two other endocytic receptors, DC-SIGN and the mannose receptor CD206, both organize in similarly ~80 nm sized domains which, upon binding to fungal pathogens, merge into larger disc-shaped clusters of 150–175 nm in diameter, and this facilitates the ingestion of the pathogen [25–28] (Box 2). Toll-like receptor 4 (TLR4) is also present in nanodomains of 60–80 nm in size, and it was demonstrated by SMLM that its oligomeric state is controlled by its ligand endotoxin and its coreceptors MD2 and CD14 [29,30]. Finally, a SMLM study of endocytic cargo revealed that the vesicular acetylcholine transporter rapidly diffuses over the membrane until it is trapped for uptake by a membrane structure that contains clathrin and its adapter protein AP2 [31].

### Role of Lipids in Receptor Clustering

The combination of SMLM and total internal reflection fluorescence (TIRF) microscopy enables the tracking of single molecules in time, and revealed that membrane clustering of **glycosylphosphatidylinositol (GPI)**-anchored receptors in the outer leaflet of the plasma membrane is promoted by transmembrane coupling to the long acyl-chain lipid phosphatidylserine in the inner leaflet [32,33]. Phosphatidylserine directly interacts with F-actin adaptors and thereby anchors the outer-leaflet receptors to the cortical actin cytoskeleton [32,33]. Several other lipid species can also contribute to receptor clustering. First, cholesterol-mediated lipid phase separation is involved in clustering of GPI-anchored proteins [33,34]. Second, domains with lactosylceramide (LacCer), a glycosphingolipid present in immune phagocytes that contributes to integrin-mediated phagocytosis, are separated from domains containing another abundant phosphatidylglucoside (PtdGlc) [35]. Finally, domain formation of the WNT receptor LNP6, clathrin, and its adaptor AP2 depend on coclustering with phosphatidylinositol 4,5-bisphosphate [$PI(4,5)P_2$] lipids [36]. Such clustering of phosphoinositides in membrane domains has been reported for several species. For instance, a SMLM study revealed that phosphatidylinositol 4-phosphate (PI4P), phosphatidylinositol 4,5-bisphosphate [$PI(4,5)P_2$] and phosphatidylinositol 3,4,5-triphosphate [$PI(3,4,5)P_3$] are all present in domains of about 350–400 nm diameter in the plasma membrane of insulin-secreting INS-1 cells [37]. Membrane domains of phosphoinositides can be highly specific because plasma membrane domains containing $PI(4,5)P_2$ can segregate from domains enriched in $PI(3,4,5)P_3$ [38].

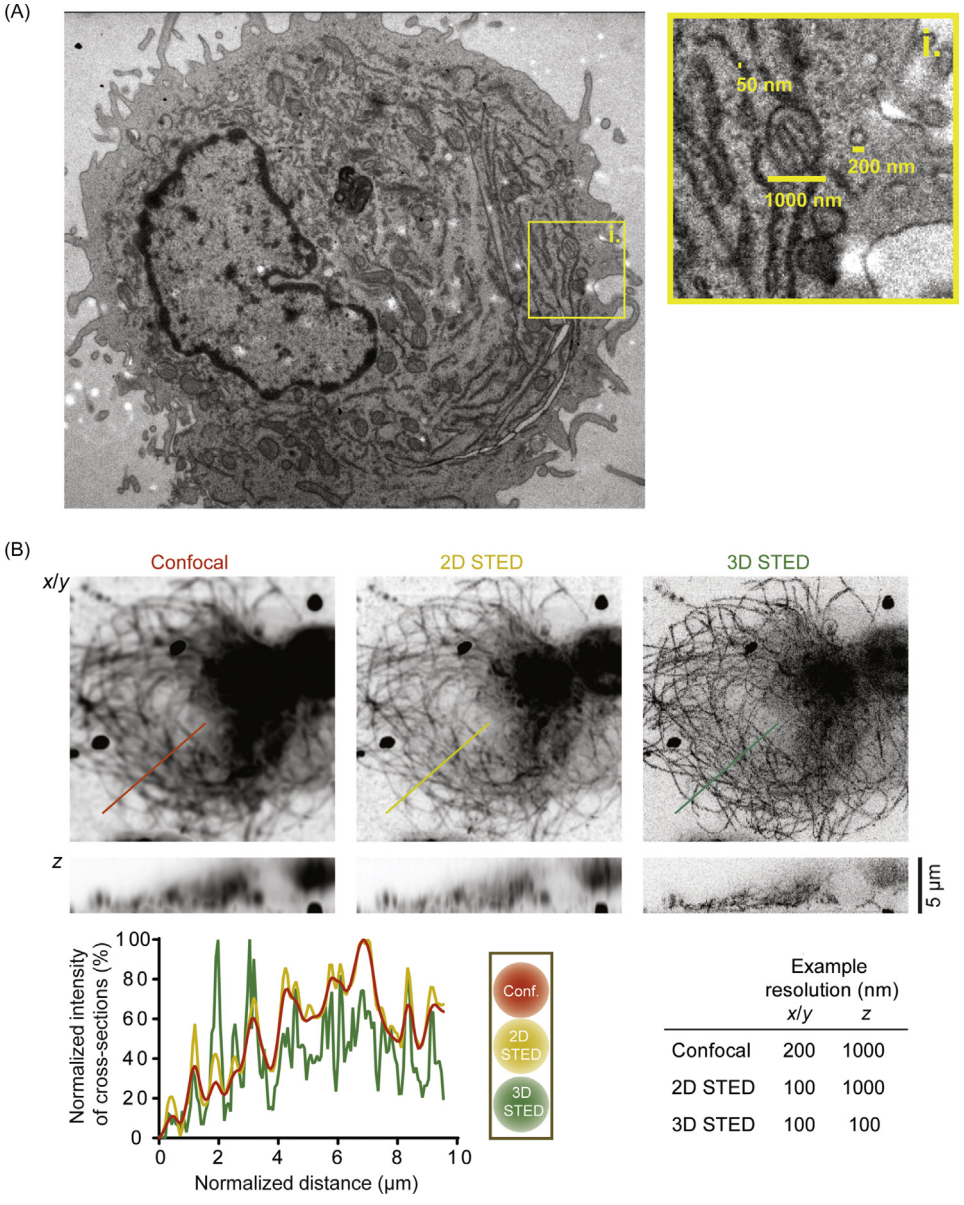


Figure 1. The Advantage of High Spatial Resolution for Resolving Cellular Structures. (A) Human blood monocyte-derived dendritic cell ultrastructure revealed by transmission electron microscopy (EM). Indicated are the approximate diffraction limited spatial resolution (~200 nm lateral, *x*/*y*; and 1000 nm axial, *z*) and an example of the 50 nm spatial resolution attainable by super-resolution microscopy. (B) Maximum intensity *z*-projection and orthogonal view of confocal, 2D stimulated emission depletion (STED), and 3D STED microscopy of dendritic cells with microtubules stained with silicon rhodamine (SiR) tubulin [114]. Cross-sections of different colors correspond to intensity profiles. Image courtesy of Alf Honigmann (Max Planck Institute for Cell Biology and Genetics, Dresden, Germany).

## Glossary

**BAR domain:** named after three proteins that contain this domain – bin/amphiphysin/rvs. BAR domains facilitate membrane curvature and/or bind to curved membranes.
**Correlative light-electron microscopy (CLEM):** overlapping fluorescence and electron microscopy images of the same specimen.
**Electron microscopy (EM):** a microscopy technique that uses electron beams of much shorter wavelength than visible light, allowing the ultrastructure of frozen or chemically fixed samples to be resolved.
**F-actin:** filamentous actin, a component of the cytoskeleton.
**Fluorescence resonance energy transfer (FRET):** enables the detection of small changes (nm) in distance between two fluorophores.
**Glycosylphosphatidylinositol (GPI):** a glycolipid that can be post-translationally coupled to the C-terminus of proteins.
**HaloTag:** 33 kDa tag derived from the bacterial enzyme haloalkane dehalogenase that can bind fluorescent dyes via a fluochloroalkane linker.
**IgG:** immunoglobulin G, a type of antibody that can be fluorescently labeled, allowing the location of specific proteins to be visualized.
**Microtubule organizing center (MTOC):** a cellular structure from which microtubules emerge.
**Soluble *N*-ethylmaleimide-sensitive factor (NSF) attachment protein receptor (SNARE):** a family of proteins that facilitate intracellular vesicle docking and fusion.

The lateral diffusion of uptake receptors can be obstructed by transmembrane proteins (so-called pickets), such as CD45 [22,39], that are immobilized by interactions with the cortical cytoskeleton. STED microscopy showed that the extracellular domain of CD45 can bind to hyaluronic acid which forms a pericellular coat and, together with the actin cytoskeleton, limits the mobility

### Box 1. Super-Resolution Microscopy Techniques

Several super-resolution microscopy techniques are now available with spatial resolutions well below the diffraction limit of conventional light microscopy. Total internal reflection fluorescence (TIRF) microscopy uses the evanescent wave of reflected light at the interface between the microscope cover glass and the specimen for excitation of fluorophores that are within ~100 nm distance of the cover glass. TIRF thereby has a high axial (*z*) resolution, whereas the lateral (*x*,*y*) resolution remains diffraction-limited. TIRF is often combined with other super-resolution microscopy techniques to achieve super-resolution in all dimensions. Stimulated emission depletion (STED) microscopy uses two laser beams of different wavelengths, one surrounding the other and creating a 'donut' [16]. The outer beam brings fluorescent molecules into a dark state of emission depletion, leaving only the fluorescent molecules in the center to actively emit photons, thereby effectively reducing the size of the excitation spot to below the diffraction limit. A second de-excitation pattern can be superimposed on the first 'donut' for combined lateral and axial super-resolution [103]. The family of single-molecule localization microscopy (SMLM) techniques uses a completely different approach and differentiates fluorophores using time [104]. The principle is to sequentially image frames with limited numbers of molecules and fit the intensity profiles of individual fluorophores. This allows the positions of these fluorophores to be obtained with localization accuracies better than the diffraction limit. By recording a large number of frames, positional information of numerous fluorophores can be combined to reconstruct a high-resolution image. High 3D resolution can be obtained by deforming the point spread function with an asymmetric lens or a deformable mirror in the emission light path. SMLM includes a range of techniques differing in the types of fluorophores used and in the methods for visualizing individual fluorophores, but the best known are photoactivatable localization microscopy (PALM) and stochastic optical reconstruction microscopy (STORM). In structured illumination microscopy (SIM), super-resolution is obtained using an overlapping pattern of excitation beams, followed by computational deconvolution. For lattice light sheet microscopy (LLSM), a planar illumination array is created by multiple beams with tightly controlled spacing oriented perpendicular to the optical light path of the emission [10]. This list is not complete, and there are other techniques for imaging below diffraction-limited resolution, for instance based on mathematical reconstruction [105,106]. Finally, fluorescence (super-resolution) microscopy can be combined with EM, which facilitates determination of the cellular localization of fluorescently labeled molecules by a technique called correlative light and electron microscopy (CLEM). Several recent reviews describe in detail the technical breakthroughs of super-resolution microscopy [9–12,16,107].

of phagocytic Fc receptors [22,39]. Such remodeling of the actin fence is necessary to enable Fc receptor clustering and the initiation of phagocytosis [22,39]. Remodeling of cortical actin is also essential for some forms of endocytosis [7] because a SIM study showed that actin rearrangements at the mammalian growth cone of neuronal axons by the F-actin bundling protein fascin are essential for endophilin-mediated endocytosis but not for clathrin-mediated endocytosis [20].

Thus, the clustering of endocytic receptors results from the interactions with various lipid species, the cortical cytoskeleton, and pericellular glycosylation. In this respect, it is similar to the clustering of proteins involved in exocytosis in distinct domains of the plasma membrane, particularly

### Box 2. Pathogen Entry

Several super-resolution microscopy studies have explored the nanostructures of the interactions of pathogens with host cells. SIM revealed that neutrophils prestore $Zn^{2+}$ in lysosomes and azurophilic granules, and utilize $Zn^{2+}$-toxicity for combating streptococcal infections [108]. Another SIM study on phagosomes formed in mouse macrophages in response to *Candida albicans* infection showed enriched SEC5 and inositol (1,4,5)-trisphosphate receptor (InsP3R) colocalization at phagosomes, and this enhanced phagocytosis and promoted antifungal signaling events [109]. Moreover, by SMLM, it was revealed how *Salmonella enterica* employs its virulence factors SifA and SseJ for endosomal tubule formation, and can thereby survive the acidic vacuoles of host cells [110]. It was found that SseJ hijacks the host motor protein kinesin for force-driven invasion along microtubules [110]. SMLM was also used to show that *Salmonella typhimurium* is surrounded by a heterogeneous coat of ubiquitin in the cytosol of host cells, with different densities of ubiquitination and of the E3 ubiquitin ligase [111]. Knockdown experiments of the host deubiquitinase OTULIN resulted in increased methionine-ubiquitin observable by SMLM microscopy, and this in turn promoted NF-κB signaling, leading to restriction of bacterial proliferation [111]. A SIM study also revealed nonhomogeneous methionine-linked ubiquitination at the surface of *S. typhimurium*, and reported a role for the ubiquitin ligase LUBAC in restricting bacterial proliferation through xenophagy and NF-κB activation [112]. Thus, super-resolution microscopy has made it possible to resolve how host ubiquitination limits the growth of *S. typhimurium*. By contrast, *Shigella flexneri*, another intracellular pathogen, expresses a protein called IpaH1.4 to negate the effect of LUBAC and promote its escape into the cytosol for survival [112]. Super-resolution microscopy has also revealed roles of ESCRT in assembly of viral particles, especially for HIV-1, as recently reviewed elsewhere [113].

**soluble *N*-ethylmaleimide-sensitive factor (NSF) attachment protein receptors (SNAREs)** (reviewed in [17]). In the future, the increasing number of colors that can be simultaneously resolved by super-resolution microscopy [40] will facilitate the characterization of the different types of membrane domains enriched in endocytic and phagocytic receptors. A largely unexplored question is how receptors are precisely organized in intracellular membranes of organelles such as early endosomes, where STED revealed cholesterol-dependent clustering of SNARE proteins [41].

## Endocytosis

### Clathrin Coat Formation

Many super-resolution microscopy studies have aimed to resolve the localization, shape, and time-dependent localization of clathrin and clathrin-associated proteins (Figure 2) [42–44]. For instance, SMLM in combination with TIRF was used to visualize the different topologies of curved clathrin-coated pits and flat clathrin plaques [44]. SIM microscopy revealed that mature clathrin-coated pits assemble as rings of about ~100 nm in diameter that persist for seconds to minutes and are associated with the actin cytoskeleton [45]. Two **correlative light-electron microscopy (CLEM)** studies mapped the arrangement of multiple endocytic proteins during various assembly stages of the clathrin coat, and showed that many proteins are primarily located near the edge (e.g., FCHO1/2, Eps15, dynamin) or the center (epsin, CALM, receptor cargo) of the clathrin lattice (Figure 2) [46,47]. Pulse-chase approaches in yeast and mammalian cells also allowed the localization of endocytic proteins to be resolved during various stages of endocytosis, and revealed that the actin-recruiting protein N-WASP is organized radially in a ring-like pattern during the early stages of clathrin pit formation, and that interactions between the clathrin coat, N-BAR proteins, and phosphoinositides orchestrate F-actin positioning at the endocytic site (Figure 2) [48–51]. Nevertheless, the role of actin in clathrin-mediated endocytosis remains controversial. Although actin might only be necessary to limit the lateral movement of endocytic vesicles in yeast [48], F-actin is already present at the base of the forming clathrin-coated vesicle [49,51], and an F-actin peak can be observed following dynamin recruitment [7,52], arguing for a function in vesicle internalization. Accordingly, a high-throughput super-resolution SMLM study in yeast showed that WASP family proteins form a ring-shaped pattern on membranes for future F-actin nucleation, and that this drives membrane invagination [51]. The latter seems to be also the case in mammalian cells because a SIM microscopy study in murine fibroblasts showed that actin can accelerate endocytosis and that clathrin-coated pit internalization is aided by actin filaments in about half of the cases [45]. A combination of TIRF and CLEM was used to visualize how clathrin coat assembly produces membrane curvature, which is the rate-limiting step for vesicle formation (Figure 2) [47]. It was found that clathrin coat assembly is versatile and accommodates membrane bending concurrently with or after the assembly of the clathrin lattice, and this bending may be regulated by axillary proteins such as CALM [47].

The process following vesicle fission and shedding of the clathrin coat has been addressed by SMLM, where it was found in yeast that the levels of phosphatidylinositol 3-phosphate (PI3P) at internalized endocytic vesicles increased 100-fold after clathrin coat shedding [53]. The yeast homolog of the early endosomal GTPase Rab5 (Vps21p) located to smaller endosomes (~80 nm-sized) at the initial stages of PI3P production, whereas the homolog of late endosomal Rab7 (Ypt7p) bound to larger endosomes (~170 nm) with more saturated PI3P levels [53]. Despite this increase in PI3P levels following endocytosis and during endosomal maturation, PI3P may already play a role during the uptake itself and in recruitment of endocytic cargo. SMLM on cultured mouse cortical neurons showed that the PI3 kinases ATM and ATR play a role in synaptic vesicle recycling and colocalize with the clathrin adaptor protein AP2, with ATR being recruited to nascent inhibitory ($VGAT^+$) and ATM to excitatory ($VGLUT^+$)

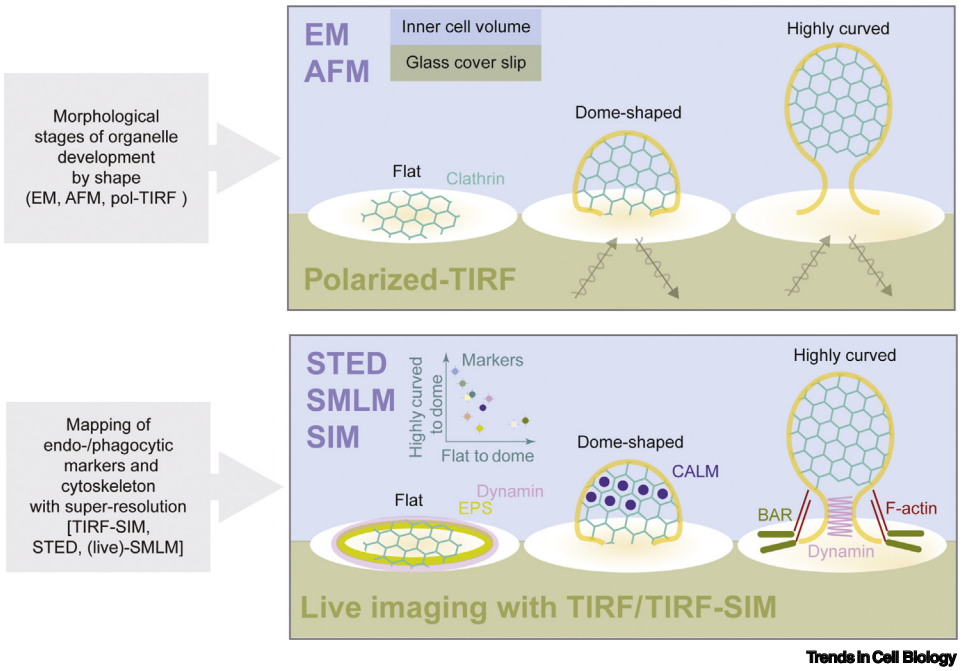


Figure 2. Coupling Membrane Curvature to Nanoscale Localization of Endocytic Proteins. (Upper panel) Electron microscopy (EM) [46,47], atomic force microscopy (AFM) [47], or polarized total internal reflection fluorescence microscopy (pol-TIRF) [47] have been used to determine the curvature of endocytic membranes. (Lower panel) Super-resolution imaging using stimulated emission depletion (STED) [50], structured illumination microscopy (SIM) [46,50], or single-molecule localization microscopy (SMLM) [43,44,46] can be coupled to the membrane curvatures determined with the methods from the upper panel. This allowed the positions of endocytic proteins (EPS, CALM, BAR-proteins, dynamin, F-actin) to be mapped during various stages of endocytosis [46,47,50].

vesicles [54]. Moreover, LLSM in SUM159 breast cancer cells expressing probes that bind clathrin and phosphoinositides revealed a new cascade of phosphoinositide lipids after fission of clathrin-coated vesicles. A pool of PI3P was already present before phosphatidylinositol (3,4)-bisphosphate (PI(3,4)$P_2$) and Rab5, and this pool was distinct from the PI3P pool of early endosomes [55].

## Caveolin Coat Formation

Super-resolution microscopy has also allowed new insights into another endocytic coat: caveolin. Although the structural organization of caveolar structures was already well understood from EM [56,57], super-resolution studies offered the possibility to image caveolae under various physiological challenges. For instance, SMLM revealed that caveolae under osmotic stress flatten and increase by ~30% in volume [58]. Although SIM and SMLM showed that caveolin oligomers can assemble in structures with different shapes (~60–80 nm diameter) [59], individual caveolae might be able to cluster in much larger (~300 nm) ribbon-like assemblies [45]. The shape and size of these caveolar structures depend on the isoform of caveolin because flask-shaped invaginating caveola are fourfold more densely packed with caveolin-1 than are flat caveola, and the density of caveolin-1 is sensitive to osmotic tensions [60]. Super-resolution microscopy also revealed signaling-mediated receptor rearrangements at caveolae, as shown by SIM for the purinergic receptor P2X7R in osteoblasts [61], by CLEM and STED for the $Ca^{2+}$ release channel ryanodine receptor at the sarcoplasmic reticulum in muscles [62,63], and by STED for the inward rectifier potassium channel Kir2.1 in human cardiac ventricles [64].

### Noncanonical Endocytosis

Endocytosis can also occur in unconventional pathways that do not depend on clathrin and caveolin. Endophilins are members of the **BAR domain** superfamily and are involved in noncanonical endocytosis in neuronal [20] and nonneuronal cells [65]. In the axon growth tips (cones) of neurons, SMLM revealed a novel form of clathrin-independent endocytosis that relies on endophilin-3 and dynamin-1, and that correlates with fascin-1-dependent F-actin bundling at the endocytic sites, and F-actin was required for retrograde trafficking of the presynaptic proteins VAMP2, SCAMP1, SV2, and synaptophysin [20]. Endophilins-A1 and A2 interact with several endocytic proteins, including dynamin, synaptojanin, and lamellipodin, and also with endocytic cargo proteins via their N-BAR or SH3 domains, leading to uptake of G protein-coupled protein receptors, receptor tyrosine kinases, and the interleukin-2 receptor [65]. Moreover, SIM revealed that endophilin-A2 reshapes membranes and, together with F-actin and dynamin, contributes to membrane scission during clathrin-independent uptake of Shiga and cholera toxins [66].

Endocytosis can be coupled to exocytosis, and this enables the rapid recycling of exocytic trafficking proteins and cellular homeostasis. STED revealed that hemifused intermediates (in which the membrane outer leaflet, but not the inner leaflet, is fused) and sometimes fully fused vesicles are able to fluctuate back to the fully separated or hemifused state [67]. This reversible transition likely resulted from a competition between membrane fusion and $Ca^{2+}$/dynamin-dependent membrane fission [67]. Other studies provided evidence for a role for dynamin in this coupling of endocytosis with exocytosis. By SIM, it was shown that dynamin controls fusion pore kinetics, promoting closure of the fusion pore, vesicle detachment from the plasmalemma, and internalization [68]. STED microscopy showed that dynamin in conjunction with the F-actin cytoskeleton led to the formation of transient fusion pores with sizes ranging up to 490 nm [69], much larger than was previously thought (<5 nm) [70,71].

### Multivesicular Body Formation

Early endosomes mature to form multivesicular bodies where the membrane is bulged into the lumen of the endosomes by the endosomal sorting complex required for transport (ESCRT) complex. This results in the formation of intraluminal vesicles which play a role in the degradation of integral membrane proteins [72]. By LLSM, it was shown that ESCRT-III subunits polymerize rapidly on yeast endosomes, together with the recruitment of at least two hexamers of the AAA ATPase Vps4 [73]. Intraluminal vesicle formation depended on ATPase activity of Vps4 and was associated with a continuous and stochastic exchange of Vps4 and ESCRT-III components [73].

## Phagocytosis

After a cell encounters a particle, a phagocytic synapse is established by formation of F-actin rich filopodia-like extensions from the membrane which engulf the particle [4]. This structure is called the phagocytic cup and creates a physical barrier for organizing the signaling cascade induced by target binding [22]. Arp2/3 complex-mediated F-actin nucleation and branching at the nascent phagosome is triggered by the GTPases Rac1, Rac2, and Cdc42, although the contribution of this actin remodeling depends on the type of phagocytosis. In case of Fc receptor-mediated phagocytosis, but not for complement C3bi receptor-mediated phagocytosis, a super-resolution microscopy study showed that branching of F-actin within lamellipodia depends on Arp2/3 [74]. By SIM on macrophages derived from Cdc42 knockout mice, it was shown that Cdc42 is dispensable for the formation of filopodia (finger-like protrusions) upon uptake of yeast particles, but is necessary for the subsequent formation of lamellipodia (the F-actin meshwork at the leading edge of a migrating cell) with parallel actin bundles during cell spreading [75].

STED microscopy was used to resolve the organization of Rac1 and actin during phagocytosis of yeast cells by dendritic cells [76]. It was found that F-actin, Rac1, and their binding protein SWAP70 align in parallel arches and sometimes in concentric rings on the surface of phagosomes [76]. In this case SWAP70 acted as an adapter, tethering the F-actin cytoskeleton to the phagocytic surface by interacting with Rac1 and phosphatidylinositol (3,4)-bisphosphate. Although structures such as actin rings or radial actin bundles for parasite internalization into host cells can already be visible by conventional confocal microscopy [77], the increased resolution of SMLM allowed the organization of such structures to be resolved and addressed the bundling of actin filaments, such as for the more accurate measurements of the dimensions of the 100 nm-sized F-actin ring during *Salmonella typhimurium* phagocytosis [78]. Although the nature of these actin rings is still unknown, they could be mediated by septins [79]. Septins control receptor and phospholipid dynamics and can form ring-like structures by bundling actin via anillin and myosin binding at the site of pathogen invasion in mammalian cells [79], structures that are reminiscent of the structures observed during phagocytosis [76]. Moreover, SMLM revealed that septins can form cables with a thickness of 20–30 nm in complex with Cdc42 and Gic1 *in vitro* [80]. However, in cells, high-resolution microscopy data on septin collars are only available for prokaryotes and budding yeast, where septins are involved in cell division and budding [80], and it would be interesting to resolve potential septin rings in phagocytosing cells by super-resolution microscopy.

## Future Technical Improvements Needed

Super-resolution microscopy has led to important new insights in endocytic trafficking, but some technical improvements are highly desirable.

### Improving Spatial Resolution

Most of the current super-resolution microscopy techniques that are widely used by biologists offer a spatial resolution between 20–60 nm lateral and about 100 nm axial, but this axial resolution is still too low to resolve complex organelle morphologies and individual endosomes. Isotropic imaging, with identical resolution in all dimensions, would be beneficial because it allows the shape and localization of 3D cellular structures to be resolved. To address this problem, new microscopy developments are increasingly improving the spatial resolution, such as MINFLUX that allows 1 nm lateral and axial resolution in live cells [81]. However, at such high microscope resolutions the size of the fluorescent probes becomes the limiting factor (Figure 3). Antibodies are several nm in size, and, although this has a negligible influence in conventional optical microscopy, it is becoming a major problem in super-resolution microscopy because it limits the spatial resolution (Figure 3) [82]. The same holds true for the ~3 nm-sized fluorescent proteins and protein tags that can specifically bind to organic fluorophores (e.g., **HaloTag** [11]). Nanobodies, that contain only a single antigen-binding fragment, may provide a partial solution to this problem because they are about twofold smaller than a full-size antibody, and the creation of a library of nanobodies with high specificities for mouse and rabbit **IgGs** is an important development [83]. Alternative approaches to replace the large fluorescent proteins are fluorescent non-natural amino acids (reviewed in [21,84,85]). The need for smaller probes has become evident in super-resolution imaging studies showing that the glutamate receptor AMPAR clusters in dynamic and transient membrane domains, instead of in the more stable domains previously observed by antibody-based labeling [86–88]. However, even organic fluorophores have a minimum physical size limit and likely cannot be made much smaller, particularly for the conjugated ring systems needed for red fluorescent dyes. Therefore, in the long run, the size of the fluorophores will become limiting for the spatial resolution of fluorescence microscopy, and other (nonfluorescent) methods would need to be developed to reach even higher spatial resolutions.

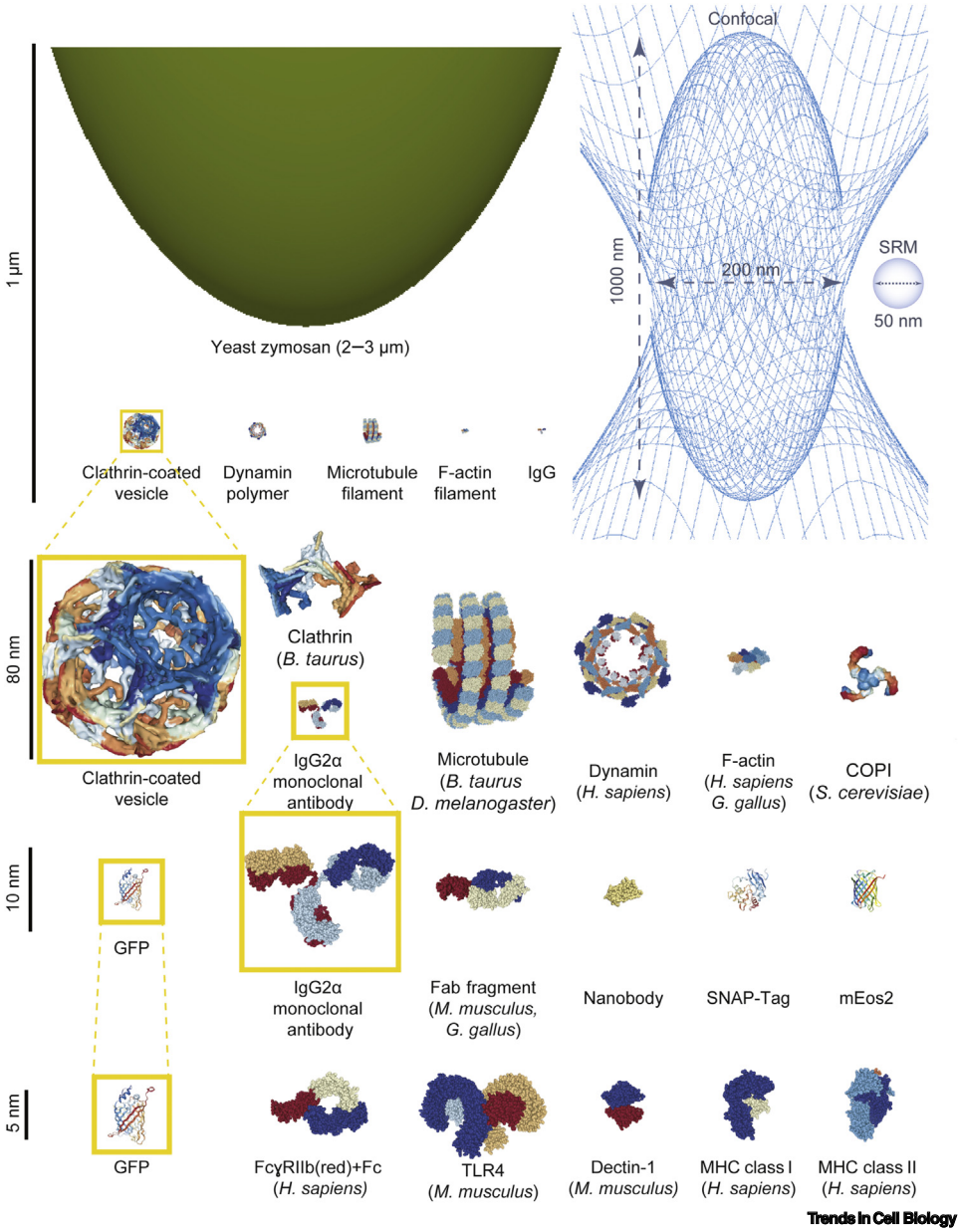


Figure 3. Spatial Scale of Phagosomes, Clathrin-Coated Vesicles, Coat Proteins, Uptake Receptors, and Probes Commonly Used in Fluorescence Super-Resolution Microscopy (SRM). All molecules and models are displayed to scale. Structures are from the Protein Data Bank (PDB): 1xi4, 3zys, 6d8c, 3j2u, 1igt, 3mkq, 1fdl, 3ogo, 5dty, 3kzy, 3s05, 2cl8, 3wjj, 3vq2, 1a1o, 3qxa. For comparison, the diffraction-limited point spread function of confocal microscopy (blue mesh) and an example of the 50 nm resolution attainable by SRM (blue ball) are shown. Abbreviations: *B. taurus, Bos taurus; D. melanogaster, Drosophila melanogaster; G. gallus, Gallus gallus; H. sapiens, Homo sapiens; M. musculus, Mus musculus; S. cerevisiae, Saccharomyces cerevisiae.*

## Improving Spectral Resolution

Most current super-resolution microscopy techniques have typically only two colors that can be discerned simultaneously. One of the reasons for this is that, in SMLM and STED, one channel

often requires more than one spectral input – the first for image acquisition and the second for fluorophore switching (localization techniques in SMLM) or because of the doughnut shape of the emission depletion beam (STED). However, resolving the nanostructure of complex molecular assemblies, such as protein complexes or organelles, requires more colors. Moreover, multiple colors would allow functional probes in super-resolution microscopy, such as ratiometric pH probes [89] or **fluorescence resonance energy transfer (FRET)** sensors for GTPases [90]. Three- and four-color STED microscopes have been developed, based on adjustable laser intensities [40] and spectral unmixing of fluorescence emission wavelengths and lifetimes [91]. SMLM can also be performed with multiple colors, for instance by careful selection of dyes and excitation schemes [92] or by sequential exchange of antibodies or probes [93,94]. These new techniques will be important for the endocytic trafficking field because they will, for instance, enable the different types of early, recycling, and late endosomes and lysosomes to be resolved.

## Improving Temporal Resolution

The low speed of image acquisition is a third limitation of current super-resolution techniques because this precludes the visualization of endo/phagosomal maturation and cytoskeletal transport (Figure 4). One issue that is apparent from this review is that most of the results discussed here have been obtained with SIM, even though this technique generally has a lower spatial resolution than either SMLM or STED. Indeed, SIM offers the advantage that it combines improved spatial resolution with a reasonably high temporal resolution (seconds), and thereby allows the dynamics of spatiotemporal recruitments, stoichiometries, and interactions between proteins and organelles to be resolved. SMLM and STED are intrinsically slow techniques because SMLM requires the acquisition of many (thousands) of images, and laser scanning in STED requires a very small pixel step to attain high spatial resolution. SIM is faster, but still requires the acquisition of multiple optical planes, and the spatial resolution of this technique is typically relatively modest compared with STED and SMLM. LLSM combines fast imaging with a high lateral and axial spatial resolution, has the additional advantage of low light exposure [10], and enables imaging of up to six colors [95], but this approach is not yet broadly available. For events at the

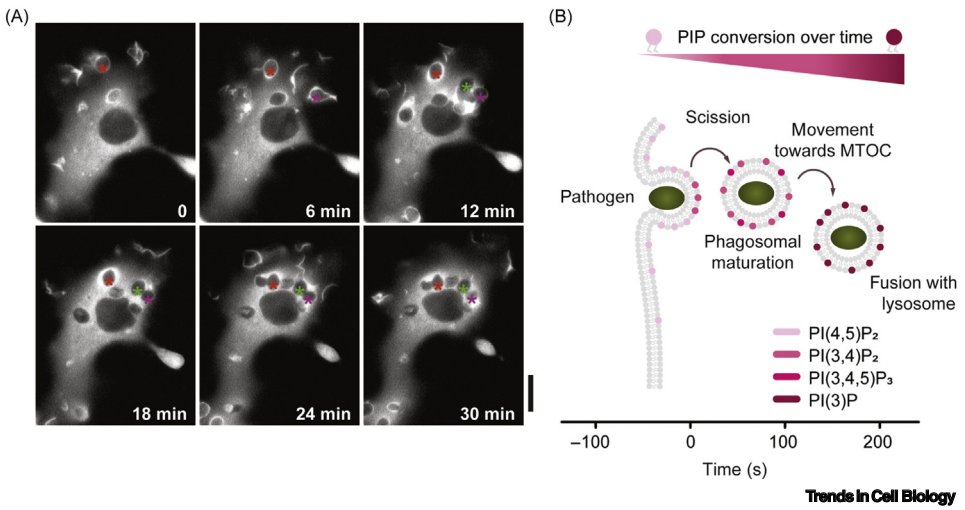


Figure 4. Temporal Resolution for Imaging of Intracellular Trafficking. (A) Confocal live cell imaging showing intracellular transport of phagosomes containing yeast particles. Individual phagosomes (labeled with stars) are transported by microtubules from the cell periphery towards the cell center over minutes after uptake. Scale bar, 10 μm. (B) Time-dependent conversion of signaling lipid phosphoinositides (PIP) during phagosomal maturation (data from [76]). Time 0 is the time of phagosomal cup sealing (i.e., complete particle ingestion). Abbreviation: min, minutes; MTOC, microtubule organizing center.

proximity of the microscopy coverslip, SIM can be combined with TIRF, thereby enabling both high spatial and temporal resolution [45]. Very recently, deconvolution approaches in combination with low photon dose and submillisecond exposure times have been developed to improve applications of SIM in live cell imaging [96]. Many other developments in super-resolution microscopy also aim to increase the speed of image acquisition, and live cell SMLM is possible now with ~10 s temporal resolution [97], for instance by 'moving-window binning' [98,99]. In SMLM, improved optics, more sensitive and faster cameras, and improved image processing algorithms [96] allow not only faster acquisition of individual frames but also higher labeling densities, reducing the number of frames necessary to compute a high-resolution image in SMLM [100]. There also are ongoing technological developments in STED, where the image acquisition rate was substantially improved by so-called parallelization, which involves scanning with optical lattices of the excitation and depletion beams [101]. All techniques will benefit from machine-learning approaches for image evaluation that allow improved resolution and prediction of structures [39,102]. These developments will allow fast events in endocytic trafficking to be resolved with not only high spatial but also temporal resolution [67–69].

## Concluding Remarks

In conclusion, super-resolution microscopy techniques have enabled the visualization of endosomal structures with nanoscale resolution, allowing membrane curvature and stages of endosome and phagosome formation to be linked with protein and lipid contents. There are still longstanding questions that will be addressable by these new techniques (see Outstanding Questions). Ongoing technological developments in super-resolution microscopy will lead to further improved spatial, temporal, and spectral resolution, enabling more applications in endocytic trafficking. Given the central role of membrane trafficking in eukaryotic cells, this will not only allow fundamental longstanding questions in cell biology to be resolved but will also lead to new understanding of the development and progression of diseases.

## Outstanding Questions

How are receptors organized in the membranes of organelles to facilitate sorting of cargo and trafficking proteins for different intracellular destinations?

What is the precise role of the F-actin cytoskeleton for different types of endocytosis?

What is the role of calcium for membrane fusion and fission in organellar trafficking?

How is membrane fusion and fission coupled in organellar trafficking?

How do membranes bend in endocytosis and organellar trafficking processes that do not involve known cage proteins?

How do lipid turnover and transfer at membrane contact sites between endosomes, the ER, and the plasma membrane contribute to endosomal maturation?

Nearly three-quarters of the 70 members of the Rab family in humans are involved in endocytic trafficking, and they play a role in endosomal maturation, coordination of vesicle budding and fusion, effector recruitment, and coordination of endosomal signaling. What are their precise localizations, interactions, and stoichiometries?

### Acknowledgments

The authors thank Alf Honigmann (Max Planck Institute for Cell Biology and Genetics, Germany), and Natalia Revelo Nuncira and Martin ter Beest (Radboud University Medical Center, the Netherlands) for microscopy images. This work was supported by a Young Investigator Grant from the Human Frontier Science Program (HFSP; RGY0080/2018) and a Vidi grant from the Netherlands Organization for Scientific Research (NWO-ALW Vidi 864.14.001).

### References

1. Sudhof, T.C. and Rothman, J.E. (2009) Membrane fusion: grappling with SNARE and SM proteins. *Science* 323, 474–477
2. Ge, L. *et al.* (2014) The protein-vesicle network of autophagy. *Curr. Opin. Cell Biol.* 29, 18–24
3. Dingjan, I. *et al.* (2018) Endosomal and phagosomal SNAREs. *Physiol. Rev.* 98, 1465–1492
4. Levin, R. *et al.* (2015) Phosphoinositides in phagocytosis and macropinocytosis. *Biochim. Biophys. Acta* 1851, 805–823
5. Rosales, C. and Uribe-Querol, E. (2017) Phagocytosis: a fundamental process in immunity. *Biomed. Res. Int.* 2017, 9042851
6. Pauwels, A.M. *et al.* (2017) Patterns, receptors, and signals: regulation of phagosome maturation. *Trends Immunol.* 38, 407–422
7. Merrifield, C.J. and Kaksonen, M. (2014) Endocytic accessory factors and regulation of clathrin-mediated endocytosis. *Cold Spring Harb. Perspect. Biol.* 6, a016733
8. Gray, M. and Botelho, R.J. (2017) Phagocytosis: hungry, hungry cells. *Meth. Mol. Biol.* 1519, 1–16
9. von Diezmann, A. *et al.* (2017) Three-dimensional localization of single molecules for super-resolution imaging and single-particle tracking. *Chem. Rev.* 117, 7244–7275
10. Liu, Z. *et al.* (2015) Imaging live-cell dynamics and structure at the single-molecule level. *Mol. Cell* 58, 644–659
11. Henriques, R. *et al.* (2011) PALM and STORM: unlocking live-cell super-resolution. *Biopolymers* 95, 322–331
12. Sezgin, E. *et al.* (2017) Polarity-sensitive probes for superresolution stimulated emission depletion microscopy. *Biophys. J.* 113, 1321–1330
13. Stone, M.B. *et al.* (2017) Super-resolution microscopy: shedding light on the cellular plasma membrane. 117, 7457–7477
14. Richter, K.N. *et al.* (2017) Review of combined isotopic and optical nanoscopy. *Neurophotonics* 4, 020901
15. Joensuu, M. and Martinez-Marmol, R. (2017) Visualizing endocytic recycling and trafficking in live neurons by subdiffractional tracking of internalized molecules. *Nat. Protoc.* 12, 2590–2622
16. Sahl, S.J. *et al.* (2017) Fluorescence nanoscopy in cell biology. *Nat. Rev. Mol. Cell Biol.* 18, 685–701
17. van den Bogaart, G. *et al.* (2013) Microdomains of SNARE proteins in the plasma membrane. *Curr. Top. Membr.* 72, 193–230
18. Rossy, J. *et al.* (2013) Super-resolution microscopy of the immunological synapse. *Curr. Opin. Immunol.* 25, 307–312
19. Garcia-Parajo, M.F. *et al.* (2014) Nanoclustering as a dominant feature of plasma membrane organization. *J. Cell Sci.* 127, 4995–5005
20. Nozumi, M. *et al.* (2017) Coordinated movement of vesicles and actin bundles during nerve growth revealed by superresolution microscopy. *Cell Rep.* 18, 2203–2216

21. Saal, K.A. *et al.* (2018) Combined use of unnatural amino acids enables dual color super-resolution imaging of proteins via click chemistry. *ACS Nano* 12, 12247–12254
22. Freeman, S.A. *et al.* (2016) Integrins form an expanding diffusional barrier that coordinates phagocytosis. *Cell* 164, 128–140
23. Shelby, S.A. *et al.* (2013) Distinct stages of stimulated FcepsilonRI receptor clustering and immobilization are identified through superresolution imaging. *Biophys. J.* 105, 2343–2354
24. Lopes, F.B. *et al.* (2017) Membrane nanoclusters of FcgammaRI segregate from inhibitory SIRPalpha upon activation of human macrophages. *J. Cell Biol.* 216, 1123–1141
25. Itano, M.S. *et al.* (2014) Super-resolution imaging of C-type lectin spatial rearrangement within the dendritic cell plasma membrane at fungal microbe contact sites. *Front. Phys.* 2, 46
26. Cambi, A. *et al.* (2004) Microdomains of the C-type lectin DC-SIGN are portals for virus entry into dendritic cells. *J. Cell Biol.* 164, 145–155
27. Koopman, M. *et al.* (2004) Near-field scanning optical microscopy in liquid for high resolution single molecule detection on dendritic cells. *FEBS Lett.* 573, 6–10
28. de Bakker, B.I. *et al.* (2007) Nanoscale organization of the pathogen receptor DC-SIGN mapped by single-molecule high-resolution fluorescence microscopy. *Chemphyschem* 8, 1473–1480
29. Krüger, C.L. *et al.* (2017) Quantitative single-molecule imaging of TLR4 reveals ligand-specific receptor dimerization. *Sci. Signal.* 10, eaan1308
30. Zeuner, M.T. *et al.* (2016) Biased signalling is an essential feature of TLR4 in glioma cells. *Biochim. Biophys. Acta* 1863, 3084–3095
31. Sochacki, K.A. *et al.* (2012) Imaging the post-fusion release and capture of a vesicle membrane protein. *Nat. Commun.* 3, 1154
32. Kusumi, A. *et al.* (2011) Hierarchical mesoscale domain organization of the plasma membrane. *Trends Biochem. Sci.* 36, 604–615
33. Raghupathy, R. *et al.* (2015) Transbilayer lipid interactions mediate nanoclustering of lipid-anchored proteins. *Cell* 161, 581–594
34. Sevcsik, E. and Schutz, G.J. (2016) With or without rafts? Alternative views on cell membranes. *Bioessays* 38, 129–139
35. Ekyalongo, R.C. *et al.* (2015) Organization and functions of glycolipid-enriched microdomains in phagocytes. *Biochim. Biophys. Acta* 1851, 90–97
36. Kim, I. *et al.* (2013) Clathrin and AP2 are required for PtdIns (4,5)P2-mediated formation of LRP6 signalosomes. *J. Cell Biol.* 200, 419–428
37. Ji, C. *et al.* (2015) Nanoscale landscape of phosphoinositides revealed by specific pleckstrin homology (PH) domains using single-molecule superresolution imaging in the plasma membrane. *J. Biol. Chem.* 290, 26978–26993
38. Wang, J. and Richards, D.A. (2012) Segregation of PIP2 and PIP3 into distinct nanoscale regions within the plasma membrane. *Biol. Open* 1, 857–862
39. Durand, A. *et al.* (2018) A machine learning approach for online automated optimization of super-resolution optical microscopy. *Nat. Commun.* 9, 5247
40. Sidenstein, S.C. *et al.* (2016) Multicolour multilevel STED nanoscopy of actin/spectrin organization at synapses. *Sci. Rep.* 6, 26725
41. Geumann, U. *et al.* (2010) Synaptic membrane proteins form stable microdomains in early endosomes. *Microsc. Res. Tech.* 73, 606–617
42. Fiolka, R. *et al.* (2012) Time-lapse two-color 3D imaging of live cells with doubled resolution using structured illumination. *Proc. Natl. Acad. Sci. U. S. A.* 109, 5311–5315
43. Jones, S.A. *et al.* (2011) Fast, three-dimensional super-resolution imaging of live cells. *Nat. Methods* 8, 499–508
44. Leyton-Puig, D. and Isogai, T. (2017) Flat clathrin lattices are dynamic actin-controlled hubs for clathrin-mediated endocytosis and signalling of specific receptors. *Nat. Commun.* 8, 16068
45. Li, D. *et al.* (2015) Extended-resolution structured illumination imaging of endocytic and cytoskeletal dynamics. *Science* 349, aab3500
46. Sochacki, K.A. *et al.* (2017) Endocytic proteins are partitioned at the edge of the clathrin lattice in mammalian cells. *Nat. Cell Biol.* 19, 352–361
47. Scott, B.L. *et al.* (2018) Membrane bending occurs at all stages of clathrin-coat assembly and defines endocytic dynamics. 9, 419
48. Berro, J. and Pollard, T.D. (2014) Local and global analysis of endocytic patch dynamics in fission yeast using a new 'temporal superresolution' realignment method. *Mol. Biol. Cell* 25, 3501–3514
49. Picco, A. *et al.* (2015) Visualizing the functional architecture of the endocytic machinery. *Elife* 4, e04535
50. Almeida-Souza, L. *et al.* (2018) A flat BAR protein promotes actin polymerization at the base of clathrin-coated pits. *Cell* 174, 325–337
51. Mund, M. *et al.* (2018) Systematic nanoscale analysis of endocytosis links efficient vesicle formation to patterned actin nucleation. *Cell* 174, 884–896
52. Merrifield, C.J. *et al.* (2002) Imaging actin and dynamin recruitment during invagination of single clathrin-coated pits. *Nat. Cell Biol.* 4, 691–698
53. Puchner, E.M. *et al.* (2013) Counting molecules in single organelles with superresolution microscopy allows tracking of the endosome maturation trajectory. *Proc. Natl. Acad. Sci. U. S. A.* 110, 16015–16020
54. Cheng, A. *et al.* (2018) ATM and ATR play complementary roles in the behavior of excitatory and inhibitory vesicle populations. *Proc. Natl. Acad. Sci. U. S. A.* 115, E292–E301
55. He, K. *et al.* (2017) Dynamics of phosphoinositide conversion in clathrin-mediated endocytic traffic. *Nature* 552, 410–414
56. Ludwig, A. *et al.* (2013) Molecular composition and ultrastructure of the caveolar coat complex. *PLoS Biol.* 11, e1001640
57. Ludwig, A. *et al.* (2016) Architecture of the caveolar coat complex. *J. Cell Sci.* 129, 3077–3083
58. Yang, L. and Scarlata, S. (2017) Super-resolution visualization of caveola deformation in response to osmotic stress. *J. Biol. Chem.* 292, 3779–3788
59. Khater, I.M. *et al.* (2018) Super resolution network analysis defines the molecular architecture of caveolae and caveolin-1 scaffolds. *Sci. Rep.* 8, 9009
60. Tachikawa, M. *et al.* (2017) Measurement of caveolin-1 densities in the cell membrane for quantification of caveolar deformation after exposure to hypotonic membrane tension. *Sci. Rep.* 7, 7794
61. Gangadharan, V. *et al.* (2015) Caveolin-1 regulates P2X7 receptor signaling in osteoblasts. *Am. J. Physiol. Cell Physiol.* 308, C41–C50
62. Wong, J. *et al.* (2013) Nanoscale distribution of ryanodine receptors and caveolin-3 in mouse ventricular myocytes: dilation of t-tubules near junctions. *Biophys. J.* 104, L22–L24
63. Wagner, E. *et al.* (2012) Stimulated emission depletion live-cell super-resolution imaging shows proliferative remodeling of T-tubule membrane structures after myocardial infarction. *Circ. Res.* 111, 402–414
64. Vaidyanathan, R. *et al.* (2018) Inward rectifier potassium channels (Kir2.x) and caveolin-3 domain-specific interaction: implications for Purkinje cell-dependent ventricular arrhythmias. *Circ. Arrhythm. Electrophysiol.* 11, e005800
65. Boucrot, E. *et al.* (2015) Endophilin marks and controls a clathrin-independent endocytic pathway. *Nature* 517, 460–465
66. Renard, H.F. *et al.* (2015) Endophilin-A2 functions in membrane scission in clathrin-independent endocytosis. *Nature* 517, 493–496
67. Zhao, W.D. *et al.* (2016) Hemi-fused structure mediates and controls fusion and fission in live cells. *Nature* 534, 548–552
68. Lasic, E. *et al.* (2017) Dynamin regulates the fusion pore of endo- and exocytotic vesicles as revealed by membrane capacitance measurements. *Biochim. Biophys. Acta* 1861, 2293–2303
69. Shin, W. *et al.* (2018) Visualization of membrane pore in live cells reveals a dynamic-pore theory governing fusion and endocytosis. *Cell* 173, 934–945
70. Kreft, M. *et al.* (2016) Unproductive exocytosis. *J. Neurochem.* 137, 880–889

71. Kreft, M. *et al.* (2018) Angstrom-size exocytotic fusion pore: implications for pituitary hormone secretion. *Mol. Cell. Endocrinol.* 463, 65–71
72. Schoneberg, J. *et al.* (2017) Reverse-topology membrane scission by the ESCRT proteins. *Nat. Rev. Mol. Cell Biol.* 18, 5–17
73. Adell, M.A.Y. and Migliano, S.M. (2017) Recruitment dynamics of ESCRT-III and Vps4 to endosomes and implications for reverse membrane budding. *eLife* 6, e31652
74. Rotty, J.D. *et al.* (2017) Arp2/3 complex is required for macrophage integrin functions but is dispensable for FcR phagocytosis and *in vivo* motility. *Dev. Cell* 42, 498–513
75. Horsthemke, M. *et al.* (2017) Multiple roles of filopodial dynamics in particle capture and phagocytosis and phenotypes of Cdc42 and Myo10 deletion. *J. Biol. Chem.* 292, 7258–7273
76. Baranov, M.V. *et al.* (2016) SWAP70 organizes the actin cytoskeleton and is essential for phagocytosis. *Cell Rep.* 17, 1518–1531
77. Jasnin, M. *et al.* (2013) Three-dimensional architecture of actin filaments in *Listeria monocytogenes* comet tails. *Proc. Natl. Acad. Sci. U. S. A.* 110, 20521–20526
78. Han, J.J. *et al.* (2014) Actin restructuring during *Salmonella typhimurium* infection investigated by confocal and super-resolution microscopy. *J. Biomed. Opt.* 19, 16011
79. Torraca, V. and Mostowy, S. (2016) Septins and bacterial infection. *Front. Cell Dev. Biol.* 4, 127
80. Kaplan, C. *et al.* (2015) Absolute arrangement of subunits in cytoskeletal septin filaments in cells measured by fluorescence microscopy. *Nano Lett.* 15, 3859–3864
81. Eilers, Y. and Ta, H. (2018) MINFLUX monitors rapid molecular jumps with superior spatiotemporal resolution. *Proc. Natl. Acad. Sci. U. S. A.* 115, 6117–6122
82. van den Bogaart, G. *et al.* (2011) Membrane protein sequestering by ionic protein–lipid interactions. *Nature* 479, 552–555
83. Pleiner, T. and Bates, M. (2018) A toolbox of anti-mouse and anti-rabbit IgG secondary nanobodies. 217, 1143–1154
84. van de Linde, S. *et al.* (2012) Live-cell super-resolution imaging with synthetic fluorophores. *Annu. Rev. Phys. Chem.* 63, 519–540
85. Lang, K. and Chin, J.W. (2014) Cellular incorporation of unnatural amino acids and bioorthogonal labeling of proteins. *Chem. Rev.* 114, 4764–4806
86. Hastings, M.H. and Man, H.Y. (2018) Synaptic capture of laterally diffusing AMPA receptors – an idea that stuck. *Trends Neurosci.* 41, 330–332
87. Nair, D. *et al.* (2013) Super-resolution imaging reveals that AMPA receptors inside synapses are dynamically organized in nanodomains regulated by PSD95. *J. Neurosci.* 33, 13204–13224
88. Lee, S.H. *et al.* (2017) Super-resolution imaging of synaptic and extra-synaptic AMPA receptors with different-sized fluorescent probes. *eLife* 6, e27744
89. Richardson, D.S. *et al.* (2017) SRpHi ratiometric pH biosensors for super-resolution microscopy. *Nat. Commun.* 8, 577
90. Hodgson, L. *et al.* (2010) Biosensors for characterizing the dynamics of rho family GTPases in living cells. *Curr. Protoc. Cell. Biol.* Chapter 14 Unit 14.11.1–26
91. Winter, F.R. *et al.* (2017) Multicolour nanoscopy of fixed and living cells with a single STED beam and hyperspectral detection. *Sci. Rep.* 7, 46492
92. Dempsey, G.T. *et al.* (2011) Evaluation of fluorophores for optimal performance in localization-based super-resolution imaging. *Nat. Methods* 8, 1027–1036
93. Jungmann, R. *et al.* (2014) Multiplexed 3D cellular super-resolution imaging with DNA-PAINT and Exchange-PAINT. *Nat. Methods* 11, 313–318
94. Yi, J. *et al.* (2016) madSTORM: a superresolution technique for large-scale multiplexing at single-molecule accuracy. *Mol. Biol. Cell* 27, 3591–3600
95. Valm, A.M. *et al.* (2017) Applying systems-level spectral imaging and analysis to reveal the organelle interactome. *Nature* 546, 162–167
96. Huang, X. *et al.* (2018) Fast, long-term, super-resolution imaging with Hessian structured illumination microscopy. *Nat. Biotechnol.* 36, 451–459
97. Zobiak, B. and Failla, A.V. (2018) Advanced spinning disk-TIRF microscopy for faster imaging of the cell interior and the plasma membrane. *J. Microsc.* 269, 282–290
98. Ishitsuka, Y. *et al.* (2015) Superresolution microscopy reveals a dynamic picture of cell polarity maintenance during directional growth. *Sci. Adv.* 1, e1500947
99. Takeshita, N. *et al.* (2017) Pulses of $Ca^{2+}$ coordinate actin assembly and exocytosis for stepwise cell extension. *Proc. Natl. Acad. Sci. U. S. A.* 114, 5701–5706
100. Takeshima, T. *et al.* (2018) A multi-emitter fitting algorithm for potential live cell super-resolution imaging over a wide range of molecular densities. *J. Microsc.* 271, 266–281
101. Yang, B. *et al.* (2014) Large parallelization of STED nanoscopy using optical lattices. *Opt. Express* 22, 5581–5589
102. Wang, H. *et al.* (2019) Deep learning enables cross-modality super-resolution in fluorescence microscopy. *Nat. Methods* 16, 103–110
103. Harke, B. *et al.* (2008) Three-dimensional nanoscopy of colloidal crystals. *Nano Lett.* 8, 1309–1313
104. Patterson, G. *et al.* (2010) Superresolution imaging using single-molecule localization. *Annu. Rev. Phys. Chem.* 61, 345–367
105. Kabbani, A.M. and Kelly, C.V. (2017) The detection of nanoscale membrane bending with polarized localization microscopy. *Biophys. J.* 113, 1782–1794
106. Horisaki, R. *et al.* (2017) Learning-based single-shot superresolution in diffractive imaging. *Appl. Opt.* 56, 8896–8901
107. Baddeley, D. and Bewersdorf, J. (2018) Biological Insight from super-resolution microscopy: what we can learn from localization-based images. *Annu. Rev. Biochem.* 87, 965–989
108. Ong, C.Y. *et al.* (2018) New insights into the role of zinc acquisition and zinc tolerance in group a streptococcal infection. *Infect. Immun.* 86, e00048-18
109. Yang, L. *et al.* (2018) InsP3R-SEC5 interaction on phagosomes modulates innate immunity to *Candida albicans* by promoting cytosolic $Ca^{2+}$ elevation and TBK1 activity. *BMC Biol.* 16, 46
110. Gao, Y. *et al.* (2018) The Pearling transition provides evidence of force-driven endosomal tubulation during *Salmonella* infection. *MBio* 9
111. van Wijk, S.J.L. *et al.* (2017) Linear ubiquitination of cytosolic *Salmonella typhimurium* activates NF-kappaB and restricts bacterial proliferation. *Nat. Microbiol.* 2, 17066
112. Noad, J. *et al.* (2017) LUBAC-synthesized linear ubiquitin chains restrict cytosol-invading bacteria by activating autophagy and NF-kappaB. *Nat. Microbiol.* 2, 17063
113. Lippincott-Schwartz, J. *et al.* (2017) A consensus view of ESCRT-mediated human immunodeficiency virus type 1 abscission. *Annu. Rev. Virol.* 4, 309–325
114. Lukinavicius, G. *et al.* (2013) A near-infrared fluorophore for live-cell super-resolution microscopy of cellular proteins. *Nat. Chem.* 5, 132–139